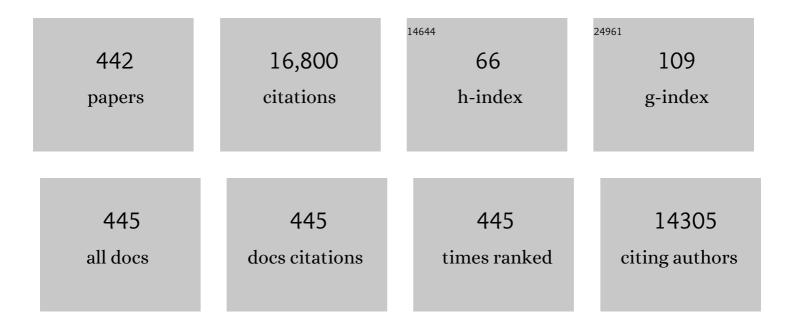
Peiyao Wang

List of Publications by Year in descending order

Source: https://exaly.com/author-pdf/5061093/publications.pdf Version: 2024-02-01



DEIVAO MANO

#	Article	IF	CITATIONS
1	Hierarchical feature representation and multimodal fusion with deep learning for AD/MCI diagnosis. NeuroImage, 2014, 101, 569-582.	2.1	732
2	Deep convolutional neural networks for multi-modality isointense infant brain image segmentation. Neurolmage, 2015, 108, 214-224.	2.1	662
3	Computer-Aided Diagnosis with Deep Learning Architecture: Applications to Breast Lesions in US Images and Pulmonary Nodules in CT Scans. Scientific Reports, 2016, 6, 24454.	1.6	488
4	Medical Image Synthesis with Context-Aware Generative Adversarial Networks. Lecture Notes in Computer Science, 2017, 10435, 417-425.	1.0	321
5	Landmark-based deep multi-instance learning for brain disease diagnosis. Medical Image Analysis, 2018, 43, 157-168.	7.0	302
6	3D conditional generative adversarial networks for high-quality PET image estimation at low dose. Neurolmage, 2018, 174, 550-562.	2.1	298
7	Hierarchical Fully Convolutional Network for Joint Atrophy Localization and Alzheimer's Disease Diagnosis Using Structural MRI. IEEE Transactions on Pattern Analysis and Machine Intelligence, 2020, 42, 880-893.	9.7	298
8	Deep Learning-Based Feature Representation for AD/MCI Classification. Lecture Notes in Computer Science, 2013, 16, 583-590.	1.0	269
9	State-space model with deep learning for functional dynamics estimation in resting-state fMRI. NeuroImage, 2016, 129, 292-307.	2.1	242
10	Deep ensemble learning of sparse regression models for brain disease diagnosis. Medical Image Analysis, 2017, 37, 101-113.	7.0	226
11	LINKS: Learning-based multi-source IntegratioN frameworK for Segmentation of infant brain images. NeuroImage, 2015, 108, 160-172.	2.1	208
12	Deep auto-context convolutional neural networks for standard-dose PET image estimation from low-dose PET/MRI. Neurocomputing, 2017, 267, 406-416.	3.5	205
13	Highâ€order restingâ€state functional connectivity network for MCI classification. Human Brain Mapping, 2016, 37, 3282-3296.	1.9	204
14	BIRNet: Brain image registration using dual-supervised fully convolutional networks. Medical Image Analysis, 2019, 54, 193-206.	7.0	199
15	A novel relational regularization feature selection method for joint regression and classification in AD diagnosis. Medical Image Analysis, 2017, 38, 205-214.	7.0	176
16	Fully convolutional networks for multi-modality isointense infant brain image segmentation. , 2016, 2016, 1342-1345.		175
17	A novel matrix-similarity based loss function for joint regression and classification in AD diagnosis. NeuroImage, 2014, 100, 91-105.	2.1	174
18	IDRiD: Diabetic Retinopathy – Segmentation and Grading Challenge. Medical Image Analysis, 2020, 59, 101561.	7.0	162

#	Article	IF	CITATIONS
19	3D Deep Learning for Multi-modal Imaging-Guided Survival Time Prediction of Brain Tumor Patients. Lecture Notes in Computer Science, 2016, 9901, 212-220.	1.0	160
20	Modeling Rett Syndrome Using TALEN-Edited MECP2 Mutant Cynomolgus Monkeys. Cell, 2017, 169, 945-955.e10.	13.5	158
21	Sparse temporally dynamic resting-state functional connectivity networks for early MCI identification. Brain Imaging and Behavior, 2016, 10, 342-356.	1.1	153
22	Estimating CT Image from MRI Data Using 3D Fully Convolutional Networks. Lecture Notes in Computer Science, 2016, 2016, 170-178.	1.0	151
23	Extraction of dynamic functional connectivity from brain grey matter and white matter for MCI classification. Human Brain Mapping, 2017, 38, 5019-5034.	1.9	151
24	Spatial Patterns, Longitudinal Development, and Hemispheric Asymmetries of Cortical Thickness in Infants from Birth to 2 Years of Age. Journal of Neuroscience, 2015, 35, 9150-9162.	1.7	148
25	Deep embedding convolutional neural network for synthesizing CT image from T1-Weighted MR image. Medical Image Analysis, 2018, 47, 31-44.	7.0	137
26	Multi-Channel 3D Deep Feature Learning for Survival Time Prediction of Brain Tumor Patients Using Multi-Modal Neuroimages. Scientific Reports, 2019, 9, 1103.	1.6	133
27	Automated detection and classification of thyroid nodules in ultrasound images using clinical-knowledge-guided convolutional neural networks. Medical Image Analysis, 2019, 58, 101555.	7.0	131
28	Evaluation of machine learning algorithms for treatment outcome prediction in patients with epilepsy based on structural connectome data. NeuroImage, 2015, 118, 219-230.	2.1	130
29	Computational neuroanatomy of baby brains: A review. NeuroImage, 2019, 185, 906-925.	2.1	125
30	Deep sparse multi-task learning for feature selection in Alzheimer's disease diagnosis. Brain Structure and Function, 2016, 221, 2569-2587.	1.2	124
31	Integration of temporal and spatial properties of dynamic connectivity networks for automatic diagnosis of brain disease. Medical Image Analysis, 2018, 47, 81-94.	7.0	123
32	Deformable Image Registration Based on Similarity-Steered CNN Regression. Lecture Notes in Computer Science, 2017, 10433, 300-308.	1.0	121
33	Interleaved 3Dâ€ <scp>CNN</scp> s for joint segmentation of smallâ€volume structures in head and neck <scp>CT</scp> images. Medical Physics, 2018, 45, 2063-2075.	1.6	119
34	Measuring the dynamic longitudinal cortex development in infants by reconstruction of temporally consistent cortical surfaces. NeuroImage, 2014, 90, 266-279.	2.1	113
35	Hierarchical fusion of features and classifier decisions for Alzheimer's disease diagnosis. Human Brain Mapping, 2014, 35, 1305-1319.	1.9	113
36	Hyper-connectivity of functional networks for brain disease diagnosis. Medical Image Analysis, 2016, 32, 84-100.	7.0	113

#	Article	IF	CITATIONS
37	View-aligned hypergraph learning for Alzheimer's disease diagnosis with incomplete multi-modality data. Medical Image Analysis, 2017, 36, 123-134.	7.0	113
38	Construction of 4D high-definition cortical surface atlases of infants: Methods and applications. Medical Image Analysis, 2015, 25, 22-36.	7.0	112
39	Estimating functional brain networks by incorporating a modularity prior. Neurolmage, 2016, 141, 399-407.	2.1	111
40	Spatial distribution and longitudinal development of deep cortical sulcal landmarks in infants. NeuroImage, 2014, 100, 206-218.	2.1	107
41	A generative probability model of joint label fusion for multi-atlas based brain segmentation. Medical Image Analysis, 2014, 18, 881-890.	7.0	107
42	Topographical Information-Based High-Order Functional Connectivity and Its Application in Abnormality Detection forÂMild Cognitive Impairment. Journal of Alzheimer's Disease, 2016, 54, 1095-1112.	1.2	103
43	Hybrid High-order Functional Connectivity Networks Using Resting-state Functional MRI for Mild Cognitive Impairment Diagnosis. Scientific Reports, 2017, 7, 6530.	1.6	102
44	Strength and similarity guided group-level brain functional network construction for MCI diagnosis. Pattern Recognition, 2019, 88, 421-430.	5.1	101
45	Adversarial learning for mono- or multi-modal registration. Medical Image Analysis, 2019, 58, 101545.	7.0	100
46	Longitudinal clinical score prediction in Alzheimer's disease with soft-split sparse regression based random forest. Neurobiology of Aging, 2016, 46, 180-191.	1.5	99
47	Integration of sparse multi-modality representation and anatomical constraint for isointense infant brain MR image segmentation. Neurolmage, 2014, 89, 152-164.	2.1	96
48	Inherent Structure-Based Multiview Learning With Multitemplate Feature Representation for Alzheimer's Disease Diagnosis. IEEE Transactions on Biomedical Engineering, 2016, 63, 1473-1482.	2.5	96
49	Hierarchical multi-atlas label fusion with multi-scale feature representation and label-specific patch partition. Neurolmage, 2015, 106, 34-46.	2.1	95
50	Multi-channel multi-scale fully convolutional network for 3D perivascular spaces segmentation in 7T MR images. Medical Image Analysis, 2018, 46, 106-117.	7.0	91
51	Resting-state functional MRI studies on infant brains: A decade of gap-filling efforts. NeuroImage, 2019, 185, 664-684.	2.1	91
52	Representation Learning: A Unified Deep Learning Framework for Automatic Prostate MR Segmentation. Lecture Notes in Computer Science, 2013, 16, 254-261.	1.0	91
53	Neurodegenerative disease diagnosis using incomplete multi-modality data via matrix shrinkage and completion. NeuroImage, 2014, 91, 386-400.	2.1	87
54	Joint feature-sample selection and robust diagnosis of Parkinson's disease from MRI data. NeuroImage, 2016, 141, 206-219.	2.1	87

#	Article	IF	CITATIONS
55	Unsupervised Deep Feature Learning for Deformable Registration of MR Brain Images. Lecture Notes in Computer Science, 2013, 16, 649-656.	1.0	85
56	Canonical feature selection for joint regression and multi-class identification in Alzheimer's disease diagnosis. Brain Imaging and Behavior, 2016, 10, 818-828.	1.1	85
57	Connectivity strengthâ€weighted sparse group representationâ€based brain network construction for M <scp>Cl</scp> classification. Human Brain Mapping, 2017, 38, 2370-2383.	1.9	85
58	Developmental topography of cortical thickness during infancy. Proceedings of the National Academy of Sciences of the United States of America, 2019, 116, 15855-15860.	3.3	82
59	Synthesizing Missing PET from MRI with Cycle-consistent Generative Adversarial Networks for Alzheimer's Disease Diagnosis. Lecture Notes in Computer Science, 2018, 11072, 455-463.	1.0	80
60	Knowledge-Guided Robust MRI Brain Extraction for Diverse Large-Scale Neuroimaging Studies on Humans and Non-Human Primates. PLoS ONE, 2014, 9, e77810.	1.1	79
61	Structured sparsity regularized multiple kernel learning for Alzheimer's disease diagnosis. Pattern Recognition, 2019, 88, 370-382.	5.1	76
62	Deep CNN ensembles and suggestive annotations for infant brain MRI segmentation. Computerized Medical Imaging and Graphics, 2020, 79, 101660.	3.5	76
63	Identification of infants at highâ€risk for autism spectrum disorder using multiparameter multiscale white matter connectivity networks. Human Brain Mapping, 2015, 36, 4880-4896.	1.9	75
64	Label-aligned multi-task feature learning for multimodal classification of Alzheimer's disease and mild cognitive impairment. Brain Imaging and Behavior, 2016, 10, 1148-1159.	1.1	72
65	Conversion and time-to-conversion predictions of mild cognitive impairment using low-rank affinity pursuit denoising and matrix completion. Medical Image Analysis, 2018, 45, 68-82.	7.0	72
66	CT male pelvic organ segmentation using fully convolutional networks with boundary sensitive representation. Medical Image Analysis, 2019, 54, 168-178.	7.0	72
67	Disrupted Brain Functional Network in Internet Addiction Disorder: A Resting-State Functional Magnetic Resonance Imaging Study. PLoS ONE, 2014, 9, e107306.	1.1	72
68	Semi-Supervised Discriminative Classification Robust to Sample-Outliers and Feature-Noises. IEEE Transactions on Pattern Analysis and Machine Intelligence, 2019, 41, 515-522.	9.7	71
69	Context-guided fully convolutional networks for joint craniomaxillofacial bone segmentation and landmark digitization. Medical Image Analysis, 2020, 60, 101621.	7.0	71
70	First-year development of modules and hubs in infant brain functional networks. NeuroImage, 2019, 185, 222-235.	2.1	70
71	Multimodal hyper-connectivity of functional networks using functionally-weighted LASSO for MCI classification. Medical Image Analysis, 2019, 52, 80-96.	7.0	66
72	Multi-site MRI harmonization via attention-guided deep domain adaptation for brain disorder identification. Medical Image Analysis, 2021, 71, 102076.	7.0	65

#	Article	IF	CITATIONS
73	Automated bone segmentation from dental CBCT images using patchâ€based sparse representation and convex optimization. Medical Physics, 2014, 41, 043503.	1.6	64
74	Matrix-Similarity Based Loss Function and Feature Selection for Alzheimer's Disease Diagnosis. , 2014, 2014, 3089-3096.		64
75	Multiâ€ŧask diagnosis for autism spectrum disorders using multiâ€modality features: A multiâ€center study. Human Brain Mapping, 2017, 38, 3081-3097.	1.9	64
76	Adversarial Similarity Network for Evaluating Image Alignment in Deep Learning Based Registration. Lecture Notes in Computer Science, 2018, 11070, 739-746.	1.0	63
77	Multiâ€atlas based representations for Alzheimer's disease diagnosis. Human Brain Mapping, 2014, 35, 5052-5070.	1.9	62
78	Deep Learning Based Inter-modality Image Registration Supervised by Intra-modality Similarity. Lecture Notes in Computer Science, 2018, 11046, 55-63.	1.0	62
79	Surface Vulnerability of Cerebral Cortex to Major Depressive Disorder. PLoS ONE, 2015, 10, e0120704.	1.1	62
80	Low-Rank Graph-Regularized Structured Sparse Regression for Identifying Genetic Biomarkers. IEEE Transactions on Big Data, 2017, 3, 405-414.	4.4	61
81	Volume-Based Analysis of 6-Month-Old Infant Brain MRI for Autism Biomarker Identification and Early Diagnosis. Lecture Notes in Computer Science, 2018, 11072, 411-419.	1.0	61
82	Dual-core steered non-rigid registration for multi-modal images via bi-directional image synthesis. Medical Image Analysis, 2017, 41, 18-31.	7.0	60
83	Multi-modal latent space inducing ensemble SVM classifier for early dementia diagnosis with neuroimaging data. Medical Image Analysis, 2020, 60, 101630.	7.0	60
84	Diagnosis of Autism Spectrum Disorders Using Temporally Distinct Restingâ€State Functional Connectivity Networks. CNS Neuroscience and Therapeutics, 2016, 22, 212-219.	1.9	59
85	Automated segmentation of dental CBCT image with prior-guided sequential random forests. Medical Physics, 2015, 43, 336-346.	1.6	58
86	Joint prediction and time estimation of COVID-19 developing severe symptoms using chest CT scan. Medical Image Analysis, 2021, 67, 101824.	7.0	58
87	Altered brain network modules induce helplessness in major depressive disorder. Journal of Affective Disorders, 2014, 168, 21-29.	2.0	57
88	Segmentation and Classification in Digital Pathology for Glioma Research: Challenges and Deep Learning Approaches. Frontiers in Neuroscience, 2020, 14, 27.	1.4	54
89	Visualization of perivascular spaces in the human brain at 7 T: sequence optimization and morphology characterization. Neurolmage, 2016, 125, 895-902.	2.1	53
90	Domain-invariant interpretable fundus image quality assessment. Medical Image Analysis, 2020, 61, 101654.	7.0	53

#	Article	IF	CITATIONS
91	Cortical thickness and surface area in neonates at high risk for schizophrenia. Brain Structure and Function, 2016, 221, 447-461.	1.2	52
92	Largeâ€scale dynamic causal modeling of major depressive disorder based on restingâ€state functional magnetic resonance imaging. Human Brain Mapping, 2020, 41, 865-881.	1.9	52
93	A toolbox for brain network construction and classification (BrainNetClass). Human Brain Mapping, 2020, 41, 2808-2826.	1.9	52
94	Prediction of standardâ€dose brain PET image by using MRI and lowâ€dose brain [¹⁸ F]FDG PET images. Medical Physics, 2015, 42, 5301-5309.	1.6	49
95	Automated quantification of cerebral edema following hemispheric infarction: Application of a machine-learning algorithm to evaluate CSF shifts on serial head CTs. NeuroImage: Clinical, 2016, 12, 673-680.	1.4	49
96	High-resolution 3D MR Fingerprinting using parallel imaging and deep learning. NeuroImage, 2020, 206, 116329.	2.1	49
97	Enhancing the representation of functional connectivity networks by fusing multiâ€view information for autism spectrum disorder diagnosis. Human Brain Mapping, 2019, 40, 833-854.	1.9	47
98	Building dynamic population graph for accurate correspondence detection. Medical Image Analysis, 2015, 26, 256-267.	7.0	46
99	Radiationâ€induced brain structural and functional abnormalities in presymptomatic phase and outcome prediction. Human Brain Mapping, 2018, 39, 407-427.	1.9	46
100	An automated method for identifying an independent component analysis-based language-related resting-state network in brain tumor subjects for surgical planning. Scientific Reports, 2017, 7, 13769.	1.6	45
101	Diagnosis of Autism Spectrum Disorder Using Central-Moment Features From Low- and High-Order Dynamic Resting-State Functional Connectivity Networks. Frontiers in Neuroscience, 2020, 14, 258.	1.4	44
102	Simultaneous Estimation of Low- and High-Order Functional Connectivity for Identifying Mild Cognitive Impairment. Frontiers in Neuroinformatics, 2018, 12, 3.	1.3	43
103	Weighted graph regularized sparse brain network construction for MCI identification. Pattern Recognition, 2019, 90, 220-231.	5.1	43
104	Synthesized 7T MRI from 3T MRI via deep learning in spatial and wavelet domains. Medical Image Analysis, 2020, 62, 101663.	7.0	43
105	Kernel-based Joint Feature Selection and Max-Margin Classification for Early Diagnosis of Parkinson's Disease. Scientific Reports, 2017, 7, 41069.	1.6	42
106	Medical Image Synthesis via Deep Learning. Advances in Experimental Medicine and Biology, 2020, 1213, 23-44.	0.8	42
107	Improved image registration by sparse patch-based deformation estimation. NeuroImage, 2015, 105, 257-268.	2.1	40
108	DesigningÂweightedÂcorrelationÂkernelsÂinÂconvolutional neural networks for functional connectivity based brain disease diagnosis. Medical Image Analysis, 2020, 63, 101709.	7.0	39

#	Article	IF	CITATIONS
109	Harmonization of Infant Cortical Thickness Using Surface-to-Surface Cycle-Consistent Adversarial Networks. Lecture Notes in Computer Science, 2019, 11767, 475-483.	1.0	39
110	Segmentation of perivascular spaces in 7 T MR image using auto-context model with orientation-normalized features. NeuroImage, 2016, 134, 223-235.	2.1	38
111	7Tâ€guided superâ€resolution of 3T MRI. Medical Physics, 2017, 44, 1661-1677.	1.6	38
112	Dilated Dense U-Net for Infant Hippocampus Subfield Segmentation. Frontiers in Neuroinformatics, 2019, 13, 30.	1.3	38
113	Spherical U-Net on Cortical Surfaces: Methods and Applications. Lecture Notes in Computer Science, 2019, 11492, 855-866.	1.0	37
114	Overall survival time prediction for high-grade glioma patients based on large-scale brain functional networks. Brain Imaging and Behavior, 2019, 13, 1333-1351.	1.1	37
115	Non-Negative Spherical Deconvolution (NNSD) for estimation of fiber Orientation Distribution Function in single-/multi-shell diffusion MRI. NeuroImage, 2014, 101, 750-764.	2.1	36
116	Discriminative multi-task feature selection for multi-modality classification of Alzheimer's disease. Brain Imaging and Behavior, 2016, 10, 739-749.	1.1	36
117	Reduced White Matter Integrity in Antisocial Personality Disorder: A Diffusion Tensor Imaging Study. Scientific Reports, 2017, 7, 43002.	1.6	36
118	Multi-task exclusive relationship learning for alzheimer's disease progression prediction with longitudinal data. Medical Image Analysis, 2019, 53, 111-122.	7.0	36
119	Subclass-based multi-task learning for Alzheimer's disease diagnosis. Frontiers in Aging Neuroscience, 2014, 6, 168.	1.7	35
120	Simultaneous and consistent labeling of longitudinal dynamic developing cortical surfaces in infants. Medical Image Analysis, 2014, 18, 1274-1289.	7.0	34
121	Locally-constrained boundary regression for segmentation of prostate and rectum in the planning CT images. Medical Image Analysis, 2015, 26, 345-356.	7.0	34
122	Identification of progressive mild cognitive impairment patients using incomplete longitudinal MRI scans. Brain Structure and Function, 2016, 221, 3979-3995.	1.2	33
123	Deep Multi-task Multi-channel Learning for Joint Classification and Regression of Brain Status. Lecture Notes in Computer Science, 2017, 10435, 3-11.	1.0	33
124	Spatiotemporal patterns of cortical fiber density in developing infants, and their relationship with cortical thickness. Human Brain Mapping, 2015, 36, 5183-5195.	1.9	32
125	Early Diagnosis of Autism Disease by Multi-channel CNNs. Lecture Notes in Computer Science, 2018, 11046, 303-309.	1.0	32
126	Graph-guided joint prediction of class label and clinical scores for the Alzheimer's disease. Brain Structure and Function, 2016, 221, 3787-3801.	1.2	31

#	Article	IF	CITATIONS
127	A Hierarchical Feature and Sample Selection Framework and Its Application for Alzheimer's Disease Diagnosis. Scientific Reports, 2017, 7, 45269.	1.6	31
128	Hierarchical High-Order Functional Connectivity Networks and Selective Feature Fusion for MCI Classification. Neuroinformatics, 2017, 15, 271-284.	1.5	31
129	Robust multi-atlas label propagation by deep sparse representation. Pattern Recognition, 2017, 63, 511-517.	5.1	31
130	Multi-View Missing Data Completion. IEEE Transactions on Knowledge and Data Engineering, 2018, 30, 1296-1309.	4.0	31
131	Construction of 4D infant cortical surface atlases with sharp folding patterns via spherical patchâ€based groupâ€wise sparse representation. Human Brain Mapping, 2019, 40, 3860-3880.	1.9	31
132	Fetal cortical surface atlas parcellation based on growth patterns. Human Brain Mapping, 2019, 40, 3881-3899.	1.9	31
133	Integrative analysis of multi-dimensional imaging genomics data for Alzheimer's disease prediction. Frontiers in Aging Neuroscience, 2014, 6, 260.	1.7	30
134	Predict brain MR image registration via sparse learning of appearance and transformation. Medical Image Analysis, 2015, 20, 61-75.	7.0	30
135	Manifold Regularized Multi-Task Feature Selection for Multi-Modality Classification in Alzheimer's Disease. Lecture Notes in Computer Science, 2013, 16, 275-283.	1.0	30
136	MRI-Based Intelligence Quotient (IQ) Estimation with Sparse Learning. PLoS ONE, 2015, 10, e0117295.	1.1	29
137	Enhancement of Perivascular Spaces in 7 T MR Image using Haar Transform of Non-local Cubes and Block-matching Filtering. Scientific Reports, 2017, 7, 8569.	1.6	29
138	Adversarial Confidence Learning for Medical Image Segmentation and Synthesis. International Journal of Computer Vision, 2020, 128, 2494-2513.	10.9	29
139	Prediction of 7â€year's conversion from subjective cognitive decline to mild cognitive impairment. Human Brain Mapping, 2021, 42, 192-203.	1.9	29
140	Outcome Prediction for Patient with High-Grade Gliomas from Brain Functional and Structural Networks. Lecture Notes in Computer Science, 2016, 9901, 26-34.	1.0	29
141	Structured Sparse Kernel Learning for Imaging Genetics Based Alzheimer's Disease Diagnosis. Lecture Notes in Computer Science, 2016, 9901, 70-78.	1.0	28
142	Morphology of perivascular spaces and enclosed blood vessels in young to middle-aged healthy adults at 7T: Dependences on age, brain region, and breathing gas. NeuroImage, 2020, 218, 116978.	2.1	28
143	Machine learning in medical imaging. Computerized Medical Imaging and Graphics, 2015, 41, 1-2.	3.5	27
144	Predicting infant cortical surface development using a 4D varifold-based learning framework and local topography-based shape morphing. Medical Image Analysis, 2016, 28, 1-12.	7.0	27

#	Article	IF	CITATIONS
145	Gyral net: A new representation of cortical folding organization. Medical Image Analysis, 2017, 42, 14-25.	7.0	27
146	Automatic brain labeling via multi-atlas guided fully convolutional networks. Medical Image Analysis, 2019, 51, 157-168.	7.0	27
147	MCI Identification by Joint Learning on Multiple MRI Data. Lecture Notes in Computer Science, 2015, 9350, 78-85.	1.0	27
148	Joint Craniomaxillofacial Bone Segmentation and Landmark Digitization by Context-Guided Fully Convolutional Networks. Lecture Notes in Computer Science, 2017, 10434, 720-728.	1.0	27
149	Automatic labeling of MR brain images by hierarchical learning of atlas forests. Medical Physics, 2016, 43, 1175-1186.	1.6	26
150	Mapping hemispheric asymmetries of the macaque cerebral cortex during early brain development. Human Brain Mapping, 2020, 41, 95-106.	1.9	26
151	Submillimeter MR fingerprinting using deep learning–based tissue quantification. Magnetic Resonance in Medicine, 2020, 84, 579-591.	1.9	26
152	A transversal approach for patch-based label fusion via matrix completion. Medical Image Analysis, 2015, 24, 135-148.	7.0	25
153	Reduced cortical thickness and increased surface area in antisocial personality disorder. Neuroscience, 2016, 337, 143-152.	1.1	25
154	Feature fusion via hierarchical supervised local CCA for diagnosis of autism spectrum disorder. Brain Imaging and Behavior, 2017, 11, 1050-1060.	1.1	25
155	Tumor Tissue Detection using Blood-Oxygen-Level-Dependent Functional MRI based on Independent Component Analysis. Scientific Reports, 2018, 8, 1223.	1.6	25
156	Robust brain ROI segmentation by deformation regression and deformable shape model. Medical Image Analysis, 2018, 43, 198-213.	7.0	25
157	Exploring folding patterns of infant cerebral cortex based on multi-view curvature features: Methods and applications. NeuroImage, 2019, 185, 575-592.	2.1	25
158	Individual identification and individual variability analysis based on cortical folding features in developing infant singletons and twins. Human Brain Mapping, 2020, 41, 1985-2003.	1.9	25
159	High-Order Graph Matching Based Feature Selection for Alzheimer's Disease Identification. Lecture Notes in Computer Science, 2013, 16, 311-318.	1.0	25
160	Joint Segmentation of Multiple Thoracic Organs in CT Images with Two Collaborative Deep Architectures. Lecture Notes in Computer Science, 2017, 10553, 21-29.	1.0	24
161	Treatment-naÃ ⁻ ve first episode depression classification based on high-order brain functional network. Journal of Affective Disorders, 2019, 256, 33-41.	2.0	24
162	Hippocampus Radiomic Biomarkers for the Diagnosis of Amnestic Mild Cognitive Impairment: A Machine Learning Method. Frontiers in Aging Neuroscience, 2019, 11, 323.	1.7	24

#	Article	IF	CITATIONS
163	Multi-task prediction of infant cognitive scores from longitudinal incomplete neuroimaging data. NeuroImage, 2019, 185, 783-792.	2.1	24
164	Mitigating gyral bias in cortical tractography via asymmetric fiber orientation distributions. Medical Image Analysis, 2020, 59, 101543.	7.0	24
165	Joint Coupled-Feature Representation and Coupled Boosting for AD Diagnosis. , 2014, 2014, 2721-2728.		23
166	Multilevel Deficiency of White Matter Connectivity Networks in Alzheimer's Disease: A Diffusion MRI Study with DTI and HARDI Models. Neural Plasticity, 2016, 2016, 1-14.	1.0	23
167	Joint prediction of longitudinal development of cortical surfaces and white matter fibers from neonatal MRI. NeuroImage, 2017, 152, 411-424.	2.1	23
168	Craniomaxillofacial Bony Structures Segmentation from MRI with Deep-Supervision Adversarial Learning. Lecture Notes in Computer Science, 2018, 11073, 720-727.	1.0	23
169	A Novel Deep Learning Framework on Brain Functional Networks for Early MCI Diagnosis. Lecture Notes in Computer Science, 2018, 11072, 293-301.	1.0	23
170	Ultra-Fast T2-Weighted MR Reconstruction Using Complementary T1-Weighted Information. Lecture Notes in Computer Science, 2018, 11070, 215-223.	1.0	23
171	Fully automatic segmentation of paraspinal muscles from 3D torso CT images via multi-scale iterative random forest classifications. International Journal of Computer Assisted Radiology and Surgery, 2018, 13, 1697-1706.	1.7	23
172	Interactive prostate segmentation using atlasâ€guided semiâ€supervised learning and adaptive feature selection. Medical Physics, 2014, 41, 111715.	1.6	22
173	Reveal Consistent Spatial-Temporal Patterns from Dynamic Functional Connectivity for Autism Spectrum Disorder Identification. Lecture Notes in Computer Science, 2016, 9900, 106-114.	1.0	22
174	Concatenated spatially-localized random forests for hippocampus labeling in adult and infant MR brain images. Neurocomputing, 2017, 229, 3-12.	3.5	22
175	RCA-U-Net: Residual Channel Attention U-Net for Fast Tissue Quantification in Magnetic Resonance Fingerprinting. Lecture Notes in Computer Science, 2019, 11766, 101-109.	1.0	22
176	Robust anatomical landmark detection with application to MR brain image registration. Computerized Medical Imaging and Graphics, 2015, 46, 277-290.	3.5	21
177	Early Diagnosis of Alzheimer's Disease by Joint Feature Selection and Classification on Temporally Structured Support Vector Machine. Lecture Notes in Computer Science, 2016, 9900, 264-272.	1.0	21
178	Learning non-linear patch embeddings with neural networks for label fusion. Medical Image Analysis, 2018, 44, 143-155.	7.0	21
179	Registration-Free Infant Cortical Surface Parcellation Using Deep Convolutional Neural Networks. Lecture Notes in Computer Science, 2018, 11072, 672-680.	1.0	21
	Noise reduction in diffusion MRI using non-local self-similar information in joint <mml:math xmlns:mml="http://www.w3.org/1998/Math/MathMI" altimg="si1.gif"</mml:math 		

180 xmlns:mml="http://www.w3.org/1998/Math/MathML" altimg="si1.gif" overflow="scroll"><mml:mrow><mml:mi>x</mml:mo>â^'</mml:mo>a^'</mml:mi>q</mml:mi></mml:mrow></mml:math>space. Medical Image Analysis, 2019, 53, 79-94.

#	Article	IF	CITATIONS
181	Learning MRI artefact removal with unpaired data. Nature Machine Intelligence, 2021, 3, 60-67.	8.3	21
182	Multi-atlas and Multi-modal Hippocampus Segmentation for Infant MR Brain Images by Propagating Anatomical Labels on Hypergraph. Lecture Notes in Computer Science, 2015, 9467, 188-196.	1.0	20
183	Multi-task feature selection via supervised canonical graph matching for diagnosis of autism spectrum disorder. Brain Imaging and Behavior, 2016, 10, 33-40.	1.1	20
184	Segmentation of Craniomaxillofacial Bony Structures from MRI with a 3D Deep-Learning Based Cascade Framework. Lecture Notes in Computer Science, 2017, 10541, 266-273.	1.0	20
185	Anatomyâ€guided joint tissue segmentation and topological correction for 6â€month infant brain MRI with risk of autism. Human Brain Mapping, 2018, 39, 2609-2623.	1.9	20
186	Improving Sparsity and Modularity of High-Order Functional Connectivity Networks for MCI and ASD Identification. Frontiers in Neuroscience, 2018, 12, 959.	1.4	20
187	Semi-supervised learning for pelvic MR image segmentation based on multi-task residual fully convolutional networks. , 2018, 2018, 885-888.		20
188	SLIR: Synthesis, localization, inpainting, and registration for image-guided thermal ablation of liver tumors. Medical Image Analysis, 2020, 65, 101763.	7.0	20
189	Low-Rank Total Variation for Image Super-Resolution. Lecture Notes in Computer Science, 2013, 16, 155-162.	1.0	20
190	Structural and Diffusion Property Alterations in Unaffected Siblings of Patients with Obsessive-Compulsive Disorder. PLoS ONE, 2014, 9, e85663.	1.1	20
191	Large deformation diffeomorphic registration of diffusion-weighted imaging data. Medical Image Analysis, 2014, 18, 1290-1298.	7.0	19
192	Estimating patientâ€specific and anatomically correct reference model for craniomaxillofacial deformity via sparse representation. Medical Physics, 2015, 42, 5809-5816.	1.6	19
193	Learning-Based Multimodal Image Registration for Prostate Cancer Radiation Therapy. Lecture Notes in Computer Science, 2016, 9902, 1-9.	1.0	19
194	Scalable joint segmentation and registration framework for infant brain images. Neurocomputing, 2017, 229, 54-62.	3.5	19
195	Low-Rank Representation for Multi-center Autism Spectrum Disorder Identification. Lecture Notes in Computer Science, 2018, 11070, 647-654.	1.0	19
196	Dual-domain convolutional neural networks for improving structural information in 3†T MRI. Magnetic Resonance Imaging, 2019, 64, 90-100.	1.0	19
197	Fusion of ULS Group Constrained High- and Low-Order Sparse Functional Connectivity Networks for MCI Classification. Neuroinformatics, 2020, 18, 1-24.	1.5	19
198	Optimal Sparse Linear Prediction for Block-missing Multi-modality Data Without Imputation. Journal of the American Statistical Association, 2020, 115, 1406-1419.	1.8	19

#	Article	IF	CITATIONS
199	Multi-task Dynamic Transformer Network for Concurrent Bone Segmentation and Large-Scale Landmark Localization with Dental CBCT. Lecture Notes in Computer Science, 2020, 12264, 807-816.	1.0	19
200	Assessing clinical progression from subjective cognitive decline to mild cognitive impairment with incomplete multi-modal neuroimages. Medical Image Analysis, 2022, 75, 102266.	7.0	19
201	Brain atlas fusion from high-thickness diagnostic magnetic resonance images by learning-based super-resolution. Pattern Recognition, 2017, 63, 531-541.	5.1	18
202	Discovering cortical sulcal folding patterns in neonates using largeâ€scale dataset. Human Brain Mapping, 2018, 39, 3625-3635.	1.9	18
203	Topological correction of infant white matter surfaces using anatomically constrained convolutional neural network. NeuroImage, 2019, 198, 114-124.	2.1	18
204	Super-resolution reconstruction of neonatal brain magnetic resonance images via residual structured sparse representation. Medical Image Analysis, 2019, 55, 76-87.	7.0	18
205	Local Diffusion Homogeneity Provides Supplementary Information in T2DM-Related WM Microstructural Abnormality Detection. Frontiers in Neuroscience, 2019, 13, 63.	1.4	18
206	Difficulty-aware hierarchical convolutional neural networks for deformable registration of brain MR images. Medical Image Analysis, 2021, 67, 101817.	7.0	18
207	A Longitudinal MRI Study of Amygdala and Hippocampal Subfields for Infants with Risk of Autism. Lecture Notes in Computer Science, 2019, 11849, 164-171.	1.0	18
208	Multi-Task Linear Programming Discriminant Analysis for the Identification of Progressive MCI Individuals. PLoS ONE, 2014, 9, e96458.	1.1	17
209	Learningâ€based subjectâ€specific estimation of dynamic maps of cortical morphology at missing time points in longitudinal infant studies. Human Brain Mapping, 2016, 37, 4129-4147.	1.9	17
210	Diagnosis of Alzheimer's Disease Using View-Aligned Hypergraph Learning with Incomplete Multi-modality Data. Lecture Notes in Computer Science, 2016, 9900, 308-316.	1.0	17
211	A learning-based CT prostate segmentation method via joint transductive feature selection and regression. Neurocomputing, 2016, 173, 317-331.	3.5	17
212	Maximum Mean Discrepancy Based Multiple Kernel Learning for Incomplete Multimodality Neuroimaging Data. Lecture Notes in Computer Science, 2017, 10435, 72-80.	1.0	17
213	Learning-based structurally-guided construction of resting-state functional correlation tensors. Magnetic Resonance Imaging, 2017, 43, 110-121.	1.0	17
214	Estimation of Brain Network Atlases Using Diffusive-Shrinking Graphs: Application to Developing Brains. Lecture Notes in Computer Science, 2017, 10265, 385-397.	1.0	17
215	Automated Segmentation of CBCT Image Using Spiral CT Atlases and Convex Optimization. Lecture Notes in Computer Science, 2013, 16, 251-258.	1.0	17
216	Cortical asymmetries in unaffected siblings of patients with obsessive–compulsive disorder. Psychiatry Research - Neuroimaging, 2015, 234, 346-351.	0.9	16

#	Article	IF	CITATIONS
217	In vivo MRI based prostate cancer localization with random forests and auto-context model. Computerized Medical Imaging and Graphics, 2016, 52, 44-57.	3.5	16
218	Learningâ€based deformable registration for infant <scp>MRI</scp> by integrating random forest with autoâ€context model. Medical Physics, 2017, 44, 6289-6303.	1.6	16
219	Joint Reconstruction and Segmentation ofÂ7T-like MR Images from 3T MRI Based onÂCascaded Convolutional Neural Networks. Lecture Notes in Computer Science, 2017, 10433, 764-772.	1.0	16
220	Learning Distance Transform for Boundary Detection and Deformable Segmentation in CT Prostate Images. Lecture Notes in Computer Science, 2014, 8679, 93-100.	1.0	16
221	Learning-Based Topological Correction for Infant Cortical Surfaces. Lecture Notes in Computer Science, 2016, 9900, 219-227.	1.0	16
222	Correlation-Weighted Sparse Group Representation for Brain Network Construction in MCI Classification. Lecture Notes in Computer Science, 2016, 9900, 37-45.	1.0	16
223	Deformable segmentation of 3D MR prostate images via distributed discriminative dictionary and ensemble learning. Medical Physics, 2014, 41, 072303.	1.6	15
224	Improving Estimation of Fiber Orientations in Diffusion MRI Using Inter-Subject Information Sharing. Scientific Reports, 2016, 6, 37847.	1.6	15
225	Disrupted functional connectome in antisocial personality disorder. Brain Imaging and Behavior, 2017, 11, 1071-1084.	1.1	15
226	Frnet: Flattened Residual Network for Infant MRI Skull Stripping. , 2019, 2019, 999-1002.		15
227	Estimating sparse functional brain networks with spatial constraints for MCI identification. PLoS ONE, 2020, 15, e0235039.	1.1	15
228	Medical Image Retrieval Using Multi-graph Learning for MCI Diagnostic Assistance. Lecture Notes in Computer Science, 2015, 9350, 86-93.	1.0	15
229	Ensemble Hierarchical High-Order Functional Connectivity Networks for MCI Classification. Lecture Notes in Computer Science, 2016, 9901, 18-25.	1.0	15
230	4D Infant Cortical Surface Atlas Construction Using Spherical Patch-Based Sparse Representation. Lecture Notes in Computer Science, 2017, 10433, 57-65.	1.0	15
231	Detail-preserving construction of neonatal brain atlases in space-frequency domain. Human Brain Mapping, 2016, 37, 2133-2150.	1.9	14
232	Can we predict subjectâ€specific dynamic cortical thickness maps during infancy from birth?. Human Brain Mapping, 2017, 38, 2865-2874.	1.9	14
233	Segmenting hippocampal subfields from 3T MRI with multi-modality images. Medical Image Analysis, 2018, 43, 10-22.	7.0	14
234	DIKA-Nets: Domain-invariant knowledge-guided attention networks for brain skull stripping of early developing macaques. NeuroImage, 2021, 227, 117649.	2.1	14

#	Article	IF	CITATIONS
235	DeepBundle: Fiber Bundle Parcellation with Graph Convolution Neural Networks. Lecture Notes in Computer Science, 2019, 11849, 88-95.	1.0	14
236	Progressive multi-atlas label fusion by dictionary evolution. Medical Image Analysis, 2017, 36, 162-171.	7.0	13
237	Constructing Multi-frequency High-Order Functional Connectivity Network for Diagnosis of Mild Cognitive Impairment. Lecture Notes in Computer Science, 2017, 10511, 9-16.	1.0	13
238	Fully automated esophagus segmentation with a hierarchical deep learning approach. , 2017, 2017, 503-506.		13
239	Unpaired Deep Cross-Modality Synthesis with Fast Training. Lecture Notes in Computer Science, 2018, 11045, 155-164.	1.0	13
240	Automatic Localization of Landmarks in Craniomaxillofacial CBCT Images Using a Local Attention-Based Graph Convolution Network. Lecture Notes in Computer Science, 2020, 12264, 817-826.	1.0	13
241	Prediction of Memory Impairment with MRI Data: A Longitudinal Study of Alzheimer's Disease. Lecture Notes in Computer Science, 2016, 9900, 273-281.	1.0	13
242	Structured Sparse Low-Rank Regression Model for Brain-Wide and Genome-Wide Associations. Lecture Notes in Computer Science, 2016, 9900, 344-352.	1.0	13
243	Feature Selection Based on Iterative Canonical Correlation Analysis for Automatic Diagnosis of Parkinson's Disease. Lecture Notes in Computer Science, 2016, 9901, 1-8.	1.0	13
244	Decoding EEG by Visual-guided Deep Neural Networks. , 2019, , .		13
245	Consistent sulcal parcellation of longitudinal cortical surfaces. NeuroImage, 2011, 57, 76-88.	2.1	12
246	Locality Adaptive Multi-modality GANs for High-Quality PET Image Synthesis. Lecture Notes in Computer Science, 2018, 11070, 329-337.	1.0	12
247	Discriminative self-representation sparse regression for neuroimaging-based alzheimer's disease diagnosis. Brain Imaging and Behavior, 2019, 13, 27-40.	1.1	12
248	Development of Dynamic Functional Architecture during Early Infancy. Cerebral Cortex, 2020, 30, 5626-5638.	1.6	12
249	Mammographic mass segmentation using multichannel and multiscale fully convolutional networks. International Journal of Imaging Systems and Technology, 2020, 30, 1095-1107.	2.7	12
250	Multi-task Learning for Neonatal Brain Segmentation Using 3D Dense-Unet with Dense Attention Guided by Geodesic Distance. Lecture Notes in Computer Science, 2019, 11795, 243-251.	1.0	12
251	Prediction of Infant MRI Appearance and Anatomical Structure Evolution Using Sparse Patch-Based Metamorphosis Learning Framework. Lecture Notes in Computer Science, 2015, 9467, 197-204.	1.0	12
252	Does Manual Delineation only Provide the Side Information in CT Prostate Segmentation?. Lecture Notes in Computer Science, 2017, 10435, 692-700.	1.0	12

#	Article	IF	CITATIONS
253	Large Deformation Image Classification Using Generalized Locality-Constrained Linear Coding. Lecture Notes in Computer Science, 2013, 16, 292-299.	1.0	12
254	Inter-modality Relationship Constrained Multi-Task Feature Selection for AD/MCI Classification. Lecture Notes in Computer Science, 2013, 16, 308-315.	1.0	12
255	A Hybrid of Deep Network and Hidden Markov Model for MCI Identification with Resting-State fMRI. Lecture Notes in Computer Science, 2015, 9349, 573-580.	1.0	11
256	Identifying High Order Brain Connectome Biomarkers via Learning on Hypergraph. Lecture Notes in Computer Science, 2016, 10019, 1-9.	1.0	11
257	Exploring diagnosis and imaging biomarkers of Parkinson's disease via iterative canonical correlation analysis based feature selection. Computerized Medical Imaging and Graphics, 2018, 67, 21-29.	3.5	11
258	Dual-Domain Cascaded Regression for Synthesizing 7T from 3T MRI. Lecture Notes in Computer Science, 2018, 11070, 410-417.	1.0	11
259	Surface-constrained volumetric registration for the early developing brain. Medical Image Analysis, 2019, 58, 101540.	7.0	11
260	Automatic Data Augmentation Via Deep Reinforcement Learning for Effective Kidney Tumor Segmentation. , 2020, , .		11
261	Multiscale neural modeling of resting-state fMRI reveals executive-limbic malfunction as a core mechanism in major depressive disorder. NeuroImage: Clinical, 2021, 31, 102758.	1.4	11
262	Hierarchical Reconstruction of 7T-like Images from 3T MRI Using Multi-level CCA and Group Sparsity. Lecture Notes in Computer Science, 2015, 9350, 659-666.	1.0	11
263	Wavelet-based Semi-supervised Adversarial Learning for Synthesizing Realistic 7T from 3T MRI. Lecture Notes in Computer Science, 2019, 11767, 786-794.	1.0	11
264	Hierarchical and symmetric infant image registration by robust longitudinalâ€exampleâ€guided correspondence detection. Medical Physics, 2015, 42, 4174-4189.	1.6	10
265	Semi-supervised Hierarchical Multimodal Feature and Sample Selection for Alzheimer's Disease Diagnosis. Lecture Notes in Computer Science, 2016, 9901, 79-87.	1.0	10
266	Functional Connectivity Network Fusion with Dynamic Thresholding for MCI Diagnosis. Lecture Notes in Computer Science, 2016, 10019, 246-253.	1.0	10
267	Robust Fusion of Diffusion MRI Data for Template Construction. Scientific Reports, 2017, 7, 12950.	1.6	10
268	Construction of spatiotemporal infant cortical surface atlas of rhesus macaque. , 2018, 2018, 704-707.		10
269	XQ-SR: Joint x-q space super-resolution with application to infant diffusion MRI. Medical Image Analysis, 2019, 57, 44-55.	7.0	10
270	Multifold Acceleration of Diffusion MRI via Deep Learning Reconstruction from Slice-Undersampled Data. Lecture Notes in Computer Science, 2019, 11492, 530-541.	1.0	10

#	Article	IF	CITATIONS
271	Low-rank dimensionality reduction for multi-modality neurodegenerative disease identification. World Wide Web, 2019, 22, 907-925.	2.7	10
272	FCN Based Label Correction for Multi-Atlas Guided Organ Segmentation. Neuroinformatics, 2020, 18, 319-331.	1.5	10
273	Joint Diagnosis and Conversion Time Prediction ofÂProgressive Mild Cognitive Impairment (pMCI) Using Low-Rank Subspace Clustering and Matrix Completion. Lecture Notes in Computer Science, 2015, 9351, 527-534.	1.0	10
274	Graph-Constrained Sparse Construction of Longitudinal Diffusion-Weighted Infant Atlases. Lecture Notes in Computer Science, 2017, 10433, 49-56.	1.0	10
275	Multidirectional and Topography-based Dynamic-scale Varifold Representations with Application to Matching Developing Cortical Surfaces. NeuroImage, 2016, 135, 152-162.	2.1	9
276	Computational medicine: A cybernetic eye for rare disease. Nature Biomedical Engineering, 2017, 1, .	11.6	9
277	Inter-Network High-Order Functional Connectivity (IN-HOFC) and its Alteration in Patients with Mild Cognitive Impairment. Neuroinformatics, 2019, 17, 547-561.	1.5	9
278	Folding drives cortical thickness variations. European Physical Journal: Special Topics, 2020, 229, 2757-2778.	1.2	9
279	Asymmetrical Multi-task Attention U-Net for the Segmentation of Prostate Bed in CT Image. Lecture Notes in Computer Science, 2020, 12264, 470-479.	1.0	9
280	Identification of Infants at Risk for Autism Using Multi-parameter Hierarchical White Matter Connectomes. Lecture Notes in Computer Science, 2015, 9352, 170-177.	1.0	9
281	Progressive Graph-Based Transductive Learning for Multi-modal Classification of Brain Disorder Disease. Lecture Notes in Computer Science, 2016, 9900, 291-299.	1.0	9
282	Multi-atlas Based Simultaneous Labeling of Longitudinal Dynamic Cortical Surfaces in Infants. Lecture Notes in Computer Science, 2013, 16, 58-65.	1.0	9
283	Multivariate Longitudinal Shape Analysis of Human Lateral Ventricles during the First Twenty-Four Months of Life. PLoS ONE, 2014, 9, e108306.	1.1	9
284	Nonlocal atlasâ€guided multiâ€channel forest learning for human brain labeling. Medical Physics, 2016, 43, 1003-1019.	1.6	8
285	Image denoising with morphology- and size-adaptive block-matching transform domain filtering. Eurasip Journal on Image and Video Processing, 2018, 2018, .	1.7	8
286	A Preliminary Volumetric MRI Study of Amygdala and Hippocampal Subfields in Autism During Infancy. , 2019, 2019, 1052-1056.		8
287	Hippocampal Segmentation From Longitudinal Infant Brain MR Images via Classification-Guided Boundary Regression. IEEE Access, 2019, 7, 33728-33740.	2.6	8
288	Segmentation of Infant Hippocampus Using Common Feature Representations Learned for Multimodal Longitudinal Data. Lecture Notes in Computer Science, 2015, 9351, 63-71.	1.0	8

#	Article	IF	CITATIONS
289	Segmentation of Perivascular Spaces Using Vascular Features and Structured Random Forest from 7T MR Image. Lecture Notes in Computer Science, 2016, 10019, 61-68.	1.0	8
290	Brain Image Labeling Using Multi-atlas Guided 3D Fully Convolutional Networks. Lecture Notes in Computer Science, 2017, 10530, 12-19.	1.0	8
291	Integration of Sparse Multi-modality Representation and Geometrical Constraint for Isointense Infant Brain Segmentation. Lecture Notes in Computer Science, 2013, 16, 703-710.	1.0	8
292	Kernel-based multi-task joint sparse classification for Alzheimer'S disease. , 2013, 2013, 1364-1367.		7
293	Predicting Alzheimer's Disease Cognitive Assessment via Robust Low-Rank Structured Sparse Model. , 2017, 2017, 3880-3886.		7
294	Construction of spatiotemporal neonatal cortical surface atlases using a large-scale dataset. , 2018, 2018, 1056-1059.		7
295	A novel approach to multiple anatomical shape analysis: Application to fetal ventriculomegaly. Medical Image Analysis, 2020, 64, 101750.	7.0	7
296	Dynamic neural circuit disruptions associated with antisocial behaviors. Human Brain Mapping, 2021, 42, 329-344.	1.9	7
297	Multi-Regression based supervised sample selection for predicting baby connectome evolution trajectory from neonatal timepoint. Medical Image Analysis, 2021, 68, 101853.	7.0	7
298	Reconstructing High-Quality Diffusion MRI Data from Orthogonal Slice-Undersampled Data Using Graph Convolutional Neural Networks. Lecture Notes in Computer Science, 2019, 11766, 529-537.	1.0	7
299	Progressive Label Fusion Framework for Multi-atlas Segmentation by Dictionary Evolution. Lecture Notes in Computer Science, 2015, 9351, 190-197.	1.0	7
300	Discovering Cortical Folding Patterns in Neonatal Cortical Surfaces Using Large-Scale Dataset. Lecture Notes in Computer Science, 2016, 9900, 10-18.	1.0	7
301	Dynamic Routing Capsule Networks for Mild Cognitive Impairment Diagnosis. Lecture Notes in Computer Science, 2019, 2019, 620-628.	1.0	7
302	Pre-operative Overall Survival Time Prediction for Glioblastoma Patients Using Deep Learning on Both Imaging Phenotype and Genotype. Lecture Notes in Computer Science, 2019, 11764, 415-422.	1.0	7
303	Machine learning in medical imaging. Machine Vision and Applications, 2013, 24, 1327-1329.	1.7	6
304	Collaborative non-local means denoising of magnetic resonance images. , 2015, 2015, 564-567.		6
305	Automatic parcellation of cortical surfaces using random forests. , 2015, 2015, 810-813.		6
306	eHUGS: Enhanced Hierarchical Unbiased Graph Shrinkage for Efficient Groupwise Registration. PLoS ONE, 2016, 11, e0146870.	1.1	6

#	Article	IF	CITATIONS
307	Learningâ€based 3T brain MRI segmentation with guidance from 7T MRI labeling. Medical Physics, 2016, 43, 6588-6597.	1.6	6
308	Inter-subject Similarity Guided Brain Network Modeling for MCI Diagnosis. Lecture Notes in Computer Science, 2017, 10541, 168-175.	1.0	6
309	Angular Upsampling in Infant Diffusion MRI Using Neighborhood Matching in x-q Space. Frontiers in Neuroinformatics, 2018, 12, 57.	1.3	6
310	Unsupervised Learning of Reference Bony Shapes for Orthognathic Surgical Planning with a Surface Deformation Network. Medical Physics, 2021, 48, 7735.	1.6	6
311	ABCnet: Adversarial bias correction network for infant brain MR images. Medical Image Analysis, 2021, 72, 102133.	7.0	6
312	Identification of MCI Using Optimal Sparse MAR Modeled Effective Connectivity Networks. Lecture Notes in Computer Science, 2013, 16, 319-327.	1.0	6
313	MRI based attenuation correction for PET/MRI via MRF segmentation and sparse regression estimated CT. , 2014, , .		5
314	Connectomics signature for characterizaton of mild cognitive impairment and schizophrenia. , 2014, 2014, 325-328.		5
315	Automatic Segmentation of Hippocampus for Longitudinal Infant Brain MR Image Sequence by Spatial-Temporal Hypergraph Learning. Lecture Notes in Computer Science, 2016, 9993, 1-8.	1.0	5
316	Exploring Gyral Patterns of Infant Cortical Folding Based on Multi-view Curvature Information. Lecture Notes in Computer Science, 2017, 10433, 12-20.	1.0	5
317	Developing Novel Weighted Correlation Kernels for Convolutional Neural Networks to Extract Hierarchical Functional Connectivities from fMRI for Disease Diagnosis. Lecture Notes in Computer Science, 2018, 11046, 1-9.	1.0	5
318	Spherical U-Net For Infant Cortical Surface Parcellation. , 2019, 2019, 1882-1886.		5
319	Deep feature descriptor based hierarchical dense matching for X-ray angiographic images. Computer Methods and Programs in Biomedicine, 2019, 175, 233-242.	2.6	5
320	Neuroimage-Based Consciousness Evaluation of Patients with Secondary Doubtful Hydrocephalus Before and After Lumbar Drainage. Neuroscience Bulletin, 2020, 36, 985-996.	1.5	5
321	Novel Effective Connectivity Network Inference for MCI Identification. Lecture Notes in Computer Science, 2017, 2017, 316-324.	1.0	5
322	New Multi-task Learning Model to Predict Alzheimer's Disease Cognitive Assessment. Lecture Notes in Computer Science, 2016, 9900, 317-325.	1.0	5
323	Estimating Reference Bony Shape Model for Personalized Surgical Reconstruction of Posttraumatic Facial Defects. Lecture Notes in Computer Science, 2019, 11768, 327-335.	1.0	5
324	Multi-stage Image Quality Assessment of Diffusion MRI via Semi-supervised Nonlocal Residual Networks. Lecture Notes in Computer Science, 2019, 11766, 521-528.	1.0	5

#	Article	IF	CITATIONS
325	Multi-Layer Multi-View Classification for Alzheimer's Disease Diagnosis. Proceedings of the AAAI Conference on Artificial Intelligence, 2018, 2018, 4406-4413.	3.6	5
326	Groupwise registration of breast DCE-MR images for accurate tumor measurement. , 2011, 2011, 598-601.		4
327	MR prostate segmentation via distributed discriminative dictionary (DDD) learning. , 2013, 2013, 868-871.		4
328	Discriminative Multi-task Feature Selection for Multi-modality Based AD/MCI Classification. , 2015, , .		4
329	Consciousness Level and Recovery Outcome Prediction Using High-Order Brain Functional Connectivity Network. Lecture Notes in Computer Science, 2017, 10511, 17-24.	1.0	4
330	Joint Robust Imputation and Classification for Early Dementia Detection Using Incomplete Multi-modality Data. Lecture Notes in Computer Science, 2018, 11121, 51-59.	1.0	4
331	Graph-Based Deep Learning forÂPrediction of Longitudinal Infant Diffusion MRI Data. Mathematics and Visualization, 2019, 2019, 133-141.	0.4	4
332	Intrinsic Patch-Based Cortical Anatomical Parcellation Using Graph Convolutional Neural Network on Surface Manifold. Lecture Notes in Computer Science, 2019, 11766, 492-500.	1.0	4
333	Anatomy-Guided Convolutional Neural Network for Motion Correction in Fetal Brain MRI. Lecture Notes in Computer Science, 2020, 12436, 384-393.	1.0	4
334	Parcellation of Infant Surface Atlas Using Developmental Trajectories of Multidimensional Cortical Attributes. Lecture Notes in Computer Science, 2015, 9351, 543-550.	1.0	4
335	A Generative Model for Resolution Enhancement of Diffusion MRI Data. Lecture Notes in Computer Science, 2013, 16, 527-534.	1.0	4
336	Incremental Learning with Selective Memory (ILSM): Towards Fast Prostate Localization for Image Guided Radiotherapy. Lecture Notes in Computer Science, 2013, 16, 378-386.	1.0	4
337	Regularized Spherical Polar Fourier Diffusion MRI with Optimal Dictionary Learning. Lecture Notes in Computer Science, 2013, 16, 639-646.	1.0	4
338	Tensorial Spherical Polar Fourier Diffusion MRI with Optimal Dictionary Learning. Lecture Notes in Computer Science, 2015, 9349, 174-182.	1.0	4
339	A Hybrid Multishape Learning Framework for Longitudinal Prediction of Cortical Surfaces and Fiber Tracts Using Neonatal Data. Lecture Notes in Computer Science, 2016, 9900, 210-218.	1.0	4
340	Alterations of dynamic redundancy of functional brain subnetworks in Alzheimer's disease and major depression disorders. NeuroImage: Clinical, 2022, 33, 102917.	1.4	4
341	Embarrassingly Parallel Acceleration of Global Tractography via Dynamic Domain Partitioning. Frontiers in Neuroinformatics, 2016, 10, 25.	1.3	3
342	Composite large margin classifiers with latent subclasses for heterogeneous biomedical data. Statistical Analysis and Data Mining, 2016, 9, 75-88.	1.4	3

#	Article	IF	CITATIONS
343	7T-Guided Learning Framework for Improving the Segmentation of 3T MR Images. Lecture Notes in Computer Science, 2016, 9901, 572-580.	1.0	3
344	Consistent Multi-Atlas Hippocampus Segmentation for Longitudinal MR Brain Images with Temporal Sparse Representation. Lecture Notes in Computer Science, 2016, 9993, 34-42.	1.0	3
345	Learning-Based 3T Brain MRI Segmentation with Guidance from 7T MRI Labeling. Lecture Notes in Computer Science, 2016, 10019, 213-220.	1.0	3
346	Joint Sparse and Low-Rank Regularized Multi-Task Multi-Linear Regression for Prediction of Infant Brain Development with Incomplete Data. Lecture Notes in Computer Science, 2017, 10433, 40-48.	1.0	3
347	Landmark-Based Alzheimer's Disease Diagnosis Using Longitudinal Structural MR Images. Lecture Notes in Computer Science, 2017, 10081, 35-45.	1.0	3
348	Multimodal Hyper-connectivity Networks for MCI Classification. Lecture Notes in Computer Science, 2017, 10433, 433-441.	1.0	3
349	Temporal Correlation Structure Learning for MCI Conversion Prediction. Lecture Notes in Computer Science, 2018, 11072, 446-454.	1.0	3
350	A computational method for longitudinal mapping of orientation-specific expansion of cortical surface in infants. Medical Image Analysis, 2018, 49, 46-59.	7.0	3
351	Cortical Foldingprints for Infant Identification. , 2019, 2019, 396-399.		3
352	Group sparse reduced rank regression for neuroimaging genetic study. World Wide Web, 2019, 22, 673-688.	2.7	3
353	6-Month Infant Brain Mri Segmentation Guided by 24-Month Data Using Cycle-Consistent Adversarial Networks. , 2020, 2020, .		3
354	Automatic Accurate Infant Cerebellar Tissue Segmentation with Densely Connected Convolutional Network. Lecture Notes in Computer Science, 2018, 11046, 233-240.	1.0	3
355	Infant Cognitive Scores Prediction with Multi-stream Attention-Based Temporal Path Signature Features. Lecture Notes in Computer Science, 2020, 12267, 134-144.	1.0	3
356	A Deep Spatial Context Guided Framework for Infant Brain Subcortical Segmentation. Lecture Notes in Computer Science, 2020, 12267, 646-656.	1.0	3
357	Disentangled Intensive Triplet Autoencoder for Infant Functional Connectome Fingerprinting. Lecture Notes in Computer Science, 2020, 12267, 72-82.	1.0	3
358	Diffusion Compartmentalization Using Response Function Groups with Cardinality Penalization. Lecture Notes in Computer Science, 2015, 9349, 183-190.	1.0	3
359	Novel Single and Multiple Shell Uniform Sampling Schemes for Diffusion MRI Using Spherical Codes. Lecture Notes in Computer Science, 2015, 9349, 28-36.	1.0	3
360	Multi-source Information Gain for Random Forest: An Application to CT Image Prediction from MRI Data. Lecture Notes in Computer Science, 2015, 9352, 321-329.	1.0	3

#	Article	IF	CITATIONS
361	Super-Resolution Reconstruction of Diffusion-Weighted Images Using 4D Low-Rank and Total Variation. Mathematics and Visualization, 2016, 2015, 15-25.	0.4	3
362	Minimizing Joint Risk of Mislabeling for Iterative Patch-Based Label Fusion. Lecture Notes in Computer Science, 2013, 16, 551-558.	1.0	3
363	Topography-Based Registration of Developing Cortical Surfaces in Infants Using Multidirectional Varifold Representation. Lecture Notes in Computer Science, 2015, 9350, 230-237.	1.0	3
364	Multi-Atlas Based Segmentation of Brainstem Nuclei from MR Images by Deep Hyper-Graph Learning. Lecture Notes in Computer Science, 2016, 9993, 51-59.	1.0	3
365	Improving Functional MRI Registration Using Whole-Brain Functional Correlation Tensors. Lecture Notes in Computer Science, 2017, 10433, 416-423.	1.0	3
366	Structural Connectivity Guided Sparse Effective Connectivity for MCI Identification. Lecture Notes in Computer Science, 2017, 10541, 299-306.	1.0	3
367	Deep Learning for Fast and Spatially-Constrained Tissue Quantification from Highly-Undersampled Data in Magnetic Resonance Fingerprinting (MRF). Lecture Notes in Computer Science, 2018, 11046, 398-405.	1.0	3
368	Deep Disentangled Hashing with Momentum Triplets for Neuroimage Search. Lecture Notes in Computer Science, 2020, 12261, 191-201.	1.0	3
369	Altered Connectedness of the Brain Chronnectome During the Progression to Alzheimer's Disease. Neuroinformatics, 2022, 20, 391-403.	1.5	3
370	Consistent 4D brain extraction of serial brain MR images. , 2013, 8669, .		2
371	Inferring functional network-based signatures via structurally-weighted LASSO model. , 2013, 2013, 970-973.		2
372	Online updating of contextâ€aware landmark detectors for prostate localization in daily treatment CT images. Medical Physics, 2015, 42, 2594-2606.	1.6	2
373	Joint labeling of multiple regions of interest (ROIS) by enhanced auto context models. , 2015, 2015, 1560-1563.		2
374	Longitudinal multi-scale mapping of infant cortical folding using spherical wavelets. , 2017, , .		2
375	A novel framework for groupwise registration of fMRI images based on common functional networks. , 2017, 2017, 485-489.		2
376	Genotype-phenotype association study via new multi-task learning model. , 2018, , .		2
377	Revealing Regional Associations of Cortical Folding Alterations with In Utero Ventricular Dilation Using Joint Spectral Embedding. Lecture Notes in Computer Science, 2018, 11072, 620-627.	1.0	2
378	Estimation of shape and growth brain network atlases for connectomic brain mapping in developing infants. , 2018, 2018, 985-989.		2

#	Article	IF	CITATIONS
379	A computational method for longitudinal mapping of orientation-specific expansion of cortical surface area in infants. , 2018, 2018, 683-686.		2
380	Fetal cortical parcellation based on growth patterns. , 2018, 2018, 696-699.		2
381	Infant brain development prediction with latent partial multi-view representation learning. , 2018, 2018, 1048-1051.		2
382	Construction of 4D Neonatal Cortical Surface Atlases Using Wasserstein Distance. , 2019, 2019, 995-998.		2
383	Hierarchical Representation For Ct Prostate Segmentation. , 2019, , .		2
384	Fast Groupwise Registration Using Multi-Level and Multi-Resolution Graph Shrinkage. Scientific Reports, 2019, 9, 12703.	1.6	2
385	Meta-Network Analysis of Structural Correlation Networks Provides Insights Into Brain Network Development. Frontiers in Human Neuroscience, 2019, 13, 93.	1.0	2
386	A Self-supervised Deep Framework forÂReference Bony Shape Estimation inÂOrthognathic Surgical Planning. Lecture Notes in Computer Science, 2021, 12904, 469-477.	1.0	2
387	Unsupervised Learning for Spherical Surface Registration. Lecture Notes in Computer Science, 2020, 12436, 373-383.	1.0	2
388	Space-Frequency Detail-Preserving Construction of Neonatal Brain Atlases. Lecture Notes in Computer Science, 2015, 9350, 255-262.	1.0	2
389	Block-Based Statistics for Robust Non-parametric Morphometry. Lecture Notes in Computer Science, 2015, 9467, 62-70.	1.0	2
390	Angular Resolution Enhancement of Diffusion MRI Data Using Inter-Subject Information Transfer. Mathematics and Visualization, 2016, 2016, 145-157.	0.4	2
391	Joint Discriminative and Representative Feature Selection for Alzheimer's Disease Diagnosis. Lecture Notes in Computer Science, 2016, 10019, 77-85.	1.0	2
392	Automatic Hippocampal Subfield Segmentation from 3T Multi-modality Images. Lecture Notes in Computer Science, 2016, 10019, 229-236.	1.0	2
393	Robust Construction of Diffusion MRI Atlases with Correction for Inter-Subject Fiber Dispersion. Mathematics and Visualization, 2017, 2016, 113-121.	0.4	2
394	Efficient Groupwise Registration for Brain MRI by Fast Initialization. Lecture Notes in Computer Science, 2017, 10541, 150-158.	1.0	2
395	A Point Says a Lot: An Interactive Segmentation Method for MR Prostate via One-Point Labeling. Lecture Notes in Computer Science, 2017, 10541, 220-228.	1.0	2
396	Image Super-Resolution by Supervised Adaption of Patchwise Self-similarity from High-Resolution Image. Lecture Notes in Computer Science, 2015, 9467, 10-18.	1.0	2

#	Article	IF	CITATIONS
397	Revealing Developmental Regionalization of Infant Cerebral Cortex Based on Multiple Cortical Properties. Lecture Notes in Computer Science, 2019, 11765, 841-849.	1.0	2
398	Identification of Abnormal Circuit Dynamics in Major Depressive Disorder via Multiscale Neural Modeling of Resting-State fMRI. Lecture Notes in Computer Science, 2019, 11766, 682-690.	1.0	2
399	Deep Granular Feature-Label Distribution Learning for Neuroimaging-Based Infant Age Prediction. Lecture Notes in Computer Science, 2019, 11767, 149-157.	1.0	2
400	A Computational Framework for Dissociating Development-Related from Individually Variable Flexibility in Regional Modularity Assignment in Early Infancy. Lecture Notes in Computer Science, 2020, 12267, 13-21.	1.0	2
401	LONGITUDINAL MULTI-SCALE MAPPING OF INFANT CORTICAL FOLDING USING SPHERICAL WAVELETS. Proceedings, 2017, 2017, 93-96.	0.0	2
402	Regularized Modal Regression with Applications in Cognitive Impairment Prediction. Advances in Neural Information Processing Systems, 2017, 30, 1448-1458.	2.8	2
403	End-to-End Dementia Status Prediction from Brain MRI Using Multi-task Weakly-Supervised Attention Network. , 2019, 11767, 158-167.		2
404	Correction to "Learning to Rank Atlases for Multiple-Atlas Segmentation―[Oct 14 1939-1953]. IEEE Transactions on Medical Imaging, 2014, 33, 2210-2210.	5.4	1
405	Detection and analysis of T2DM biomarkers from brain MR images using BrainLab. , 2014, , .		1
406	Tailor the longitudinal anaysis for nih longitudinal normal brain developmental study. , 2014, 2014, 1206-1209.		1
407	Multi-atlas Based Segmentation Editing with Interaction-Guided Constraints. Lecture Notes in Computer Science, 2015, 9351, 198-206.	1.0	1
408	Accelerating Global Tractography Using Parallel Markov Chain Monte Carlo. Mathematics and Visualization, 2016, 2016, 121-130.	0.4	1
409	Subject-Specific Estimation of Missing Cortical Thickness Maps in Developing Infant Brains. Lecture Notes in Computer Science, 2016, 9601, 83-92.	1.0	1
410	A dynamic tree-based registration could handle possible large deformations among MR brain images. Computerized Medical Imaging and Graphics, 2016, 52, 1-7.	3.5	1
411	Learning Pairwise-Similarity Guided Sparse Functional Connectivity Network for MCI Classification. , 2017, 2017, 917-922.		1
412	A Novel Image-Specific Transfer Approach for Prostate Segmentation in MR Images. , 2018, 2018, 806-810.		1
413	Skull Segmentation from CBCT Images via Voxel-Based Rendering. Lecture Notes in Computer Science, 2021, 12966, 615-623.	1.0	1
414	LATEST: Local AdapTivE and Sequential Training for Tissue Segmentation of Isointense Infant Brain MR Images. Lecture Notes in Computer Science, 2017, 2017, 26-34.	1.0	1

#	Article	IF	CITATIONS
415	Predictive Models of Resting State Networks for Assessment of Altered Functional Connectivity in MCI. Lecture Notes in Computer Science, 2013, 16, 674-681.	1.0	1
416	Inherent Structure-Guided Multi-view Learning for Alzheimer's Disease and Mild Cognitive Impairment Classification. Lecture Notes in Computer Science, 2015, 9352, 296-303.	1.0	1
417	Soft-Split Random Forest for Anatomy Labeling. Lecture Notes in Computer Science, 2015, 9352, 17-25.	1.0	1
418	lsointense Infant Brain Segmentation by Stacked Kernel Canonical Correlation Analysis. Lecture Notes in Computer Science, 2015, 9467, 28-36.	1.0	1
419	Developmental Patterns Based Individualized Parcellation of Infant Cortical Surface. Lecture Notes in Computer Science, 2017, 10433, 66-74.	1.0	1
420	Sparse Multi-view Task-Centralized Learning for ASD Diagnosis. Lecture Notes in Computer Science, 2017, 10541, 159-167.	1.0	1
421	Fusion of High-Order and Low-Order Effective Connectivity Networks for MCI Classification. Lecture Notes in Computer Science, 2017, 2017, 307-315.	1.0	1
422	Construction of Spatiotemporal Infant Cortical Surface Functional Templates. Lecture Notes in Computer Science, 2020, 12267, 238-248.	1.0	1
423	Cerebellum Tissue Segmentation with Ensemble Sparse Learning. Proceedings of the International Society for Magnetic Resonance in Medicine Scientific Meeting and Exhibition., 2017, 25, .	0.5	1
424	Automatic Segmentation of 3D Perivascular Spaces in 7T MR Images Using Multi-Channel Fully Convolutional Network. Proceedings of the International Society for Magnetic Resonance in Medicine Scientific Meeting and Exhibition., 2018, 2018, .	0.5	1
425	Non-rigid Brain MRI Registration Using Two-stage Deep Perceptive Networks. Proceedings of the International Society for Magnetic Resonance in Medicine Scientific Meeting and Exhibition., 2018, 2018, .	0.5	1
426	Inter-group image registration by hierarchical graph shrinkage. , 2013, 2013, 1030-1033.		0
427	Cortical Surface-Based Construction of Individual Structural Network with Application to Early Brain Development Study. Lecture Notes in Computer Science, 2015, 9351, 560-568.	1.0	Ο
428	Prostate deformation from inflatable rectal probe cover and dosimetric effects in prostate seed implant brachytherapy. Medical Physics, 2016, 43, 6569-6576.	1.6	0
429	Efficient Groupwise Registration of MR Brain Images via Hierarchical Graph Set Shrinkage. Lecture Notes in Computer Science, 2018, 11070, 819-826.	1.0	Ο
430	Longitudinal Sparse Regression for Neuroimage Based Consciousness Assessing and Tracking of Hydrocephalus Patients. , 2018, , .		0
431	Charting Development-Based Joint Parcellation Maps Of Human and Macaque Brains During Infancy. , 2019, 2019, 422-425.		0
432	Harnessing Group-Sparsity Regularization for Resolution Enhancement of Lung 4D-CT. Lecture Notes in Computer Science, 2013, 16, 139-146.	1.0	0

#	Article	IF	CITATIONS
433	Non-local Atlas-guided Multi-channel Forest Learning for Human Brain Labeling. Lecture Notes in Computer Science, 2015, 9351, 719-726.	1.0	0
434	Hierarchical Multi-modal Image Registration by Learning Common Feature Representations. Lecture Notes in Computer Science, 2015, 9352, 203-211.	1.0	0
435	Abstract T P45: Automated CSF Segmentation to Quantify Cerebral Edema Following Large Hemispheric Ischemic Stroke. Stroke, 2015, 46, .	1.0	0
436	Regression Guided Deformable Models for Segmentation of Multiple Brain ROIs. Lecture Notes in Computer Science, 2016, 10019, 237-245.	1.0	0
437	Automatic Cystocele Severity Grading in Ultrasound by Spatio-Temporal Regression. Lecture Notes in Computer Science, 2016, 9901, 247-255.	1.0	Ο
438	Dual-Layer Groupwise Registration for Consistent Labeling of Longitudinal Brain Images. Lecture Notes in Computer Science, 2016, 10019, 69-76.	1.0	0
439	Abstract WMP20: Validation of an Efficient Machine-learning Approach to Quantify CSF Volume Changes Using Multicenter CT Scans. Stroke, 2016, 47, .	1.0	0
440	Learning-Based Estimation of Functional Correlation Tensors in White Matter for Early Diagnosis of Mild Cognitive Impairment. Lecture Notes in Computer Science, 2017, 10530, 65-73.	1.0	0
441	Pelvic Organ Segmentation with Sample Attention based Stochastic Connection Networks. Proceedings of the International Society for Magnetic Resonance in Medicine Scientific Meeting and Exhibition., 2018, 2018, .	0.5	0
442	Reconstruction in deep learning of highly under-sampled T2-weighted image with T1-weighted image. Proceedings of the International Society for Magnetic Resonance in Medicine Scientific Meeting and Exhibition., 2018, 2018, .	0.5	0